Numerical Investigation of Transport Processes in Porous Media under Laminar, Transitional and Turbulent Flow Conditions with the Lattice-Boltzmann Method*

Tobit Flatscher[0000−0002−9790−6508], René Prieler✉[0000−0003−0102−471X], and Christoph Hochenauer[0000−0001−8739−5217]

Institute of Thermal Engineering, Graz University of Technology,
Inffeldgasse 25/B, 8010 Graz, Austria
rene.prieler@tugraz.at

Abstract. In the present paper the mass transfer in porous media under laminar, transitional and turbulent flow conditions was investigated using the *lattice-Boltzmann method (LBM)*. While previous studies have applied the LBM to species transport in complex geometries under laminar conditions, the main objective of this study was to demonstrate its applicability to *turbulent internal flows* including the *transport of a scalar quantity*. Thus, besides the resolved scalar transport, an additional turbulent diffusion coefficient was introduced to account for the subgrid-scale turbulent transport. A *packed-bed of spheres* and an *adsorber geometry based on μCT scans* were considered. While a two-relaxation time (TRT) model was applied to the laminar and transitional cases, the Bhatnagar-Gross-Krook (BGK) collision operator in conjunction with the Smagorinsky turbulence model was used for the turbulent flow regime. To validate the LBM results, simulations under the same conditions were carried out with ANSYS Fluent v19.2. It was found that the *pressure drop* over the height of the packed-bed were in close accordance to empirical correlations. Furthermore, the comparison of the calculated *species concentrations* for all flow regimes showed good agreement between the LBM and the results obtained with Ansys Fluent. Subsequently, the proposed extension of the Smagorinsky turbulence model seems to be able to predict the scalar transport under turbulent conditions.

Keywords: Turbulent scalar transport · Lattice-Boltzmann method · Porous media · Laminar flow · Turbulent flow · Turbulent relaxation time

* We sincerely thank *Markus Pieber* for the PBG simulation and his assistance with the Fluent finite-volume simulations as well as *Dr. Bernd Oberdorfer* from Österreichisches Gießerei-Institut (ÖGI), Leoben (Austria), for the generation of the raw μCT scans. This work was financially supported by the *Austrian Research Promotion Agency (FFG)*, 'Simulation der Wärmetransportvorgänge in Hochtemperaturprozessen und porösen Medien mittels lattice-Boltzmann Methode' (project 872619, eCall 22609361).

ICCS Camera Ready Version 2021
To cite this paper please use the final published version:
DOI: 10.1007/978-3-030-77980-1_19

1 Introduction

In the chemical and process industry, as well as energy applications, porous media are widely used to ensure that chemical reactions, species transport and heat transfer meet certain specifications. Tubular fixed-bed reactors are a common reactor type, where cylindrical tubes filled with catalyst pellets are continuously flowed through by a (reactive) fluid. In the process the fluid takes part in endothermic (exothermic) surface reactions that require an effective heat transfer into (out of) the system. The designer wishes to understand, quantify and control the chemical and physical phenomena inside the porous media in order to maintain a stable process. Over the last decade numerical methods have established themselves as effective tools to obtain estimates and partial insight into isolated phenomena and simplified processes that can't be directly accessed by experiments. In particular simulations of fluid flows through fully resolved geometries using Computational Fluid Dynamics (CFD) may contribute to a more fundamental understanding of the topic by taking local flow effects and their impact on the reaction process into account. [17] Such methods may be used to determine the effect of particles and their arrangement on macroscopic phenomena such as heat transfer, pressure drop, axial dispersion, surface reactions etc. Traditionally a fluid is modelled as a continuum - a dense viscous bulk - that is dominated by the conservation of mass, momentum and energy on a macroscopic level - and may be described by non-linear partial differential equations in the macroscopic unknowns, the Navier-Stokes equations. For an *incompressible Newtonian fluid* ($\rho = const.$), which is assumed for the rest of this paper, the energy equation decouples to a simple advection-diffusion equation and the mass and momentum conservation equations take a very favourable form:

$$\sum_{j\in\mathcal{D}} \frac{\partial u_j}{\partial x_j} = 0 \quad \text{(1a)} \qquad \frac{\partial u_i}{\partial t} + \sum_{j\in\mathcal{D}} u_j \frac{\partial u_i}{\partial x_j} = -\frac{1}{\rho}\frac{\partial p}{\partial x_i} + \sum_{j\in\mathcal{D}} \frac{\partial}{\partial x_j}\left(\nu \frac{\partial u_i}{\partial x_j}\right) \quad \text{(1b)}$$

For a numerical simulation the governing equations the continuous equations have to be transformed into a system of algebraic equation by discretising in time and space. Although *conventional CFD methods*, such as the finite volume method (FVM) on unstructured grids, have become a standard, they have several *limitations* in particular in modelling microscopic phenomena, grid generation for complex geometries as well as regarding computational speed and parallel scalability.

Over the years multiple particle-based methods have emerged, where the fluid is represented by discrete particles in the form of single atoms, molecules or artificial clusters of molecules instead of a continuum that interact on a short range with each other. One of the most prominent, the *incompressible lattice Boltzmann method (LBM)* was *initially investigated* in this context by several authors as an alternative to directly continuum-based methods due to its flexibility and computational efficiency. In particular Zeiser et al. initially investigated flows through porous beds of spherical particles at low Reynolds numbers [26,8] with the basic Bhatnagar-Gross-Krook (BGK) collision operator, [2] that suffers

ICCS Camera Ready Version 2021
To cite this paper please use the final published version:
DOI: 10.1007/978-3-030-77980-1_19

from a viscosity dependent wall position and instabilities for higher Reynolds (Re) numbers, but it was soon discarded due to the lack of a consistent inclusion of heat transfer as well as the *inherently transient nature* and therefore, an unjustifiable computational burden for steady-state creeping flows. Since then only Caulkin et al. have investigated the LBM for flows with non-spherical particles [4] and thus, *high-Reynolds number flows through porous beds with the LBM have never been considered*. With the advent of LBM large-eddy turbulent models [16] and novel collision operators, such as the entropic [18] and cumulant [9] collision operators, the simulation of turbulent external fluid flows using the LBM has made significant advances in recent years. Some of the resulting studies also included the *turbulent* transport of a scalar quantity (e.g. [25]) but - to the best of the authors' knowledge - in all previous studies this was implemented through a coupled Finite Difference Method (FDM) simulation.

1.1 Objectives of the Present Study

Contrary to the aforementioned publications the present paper tried to demonstrate the abilities of LBM to predict the transitional and turbulent fluid flow and species transport in realistic porous geometries. Laminar, transitional and turbulent conditions were considered in order to point out that *modern LBM is not limited to low Reynolds numbers*. Instead in particular its application to *turbulent flows in porous media is computationally very attractive* and can be carried out on consumer-grade hardware. In the process we went on to illustrate that the *additional turbulent transport of a scalar quantity can be considered directly in LBM* by coupling a second population for advection-diffusion to the hydrodynamic population with a turbulent Schmidt number. This way it is not necessary to implement a FDM solver but instead most of the LBM code can be re-used.
The present paper is therefore structured as follows: The brief introduction to the numerical modelling with LBM including the used LES model (section 2) is followed by a short paragraph about the particle Reynolds number and the considered packed-beds (section 3). Then the numerical simulation of the fluid flow and species transport under laminar, transitional and turbulent conditions in the packed-bed of spheres is discussed and results obtained by LBM are compared to ones from commercial FVM code (section 4.1). Finally in section 4.2 a simple trick is presented in order to increase the simulation domain of a realistic adsorber bed and as a proof of concept a realistic porous adsorber bed with a tube-to-particle ratio of $r_{tp} \approx 13.39$ is investigated (section 4.2).

2 Numerical Approach - Incompressible Lattice-Boltzmann Method

2.1 LBM for Computational Fluid Dynamics

Ludwig Boltzmann introduced an evolution equation for dilute gases based on an extended concept of density, the single-particle probability distribution

ICCS Camera Ready Version 2021
To cite this paper please use the final published version:
DOI: 10.1007/978-3-030-77980-1_19

$f(\boldsymbol{x}, \boldsymbol{\xi}, t) := \frac{dN_p}{d\boldsymbol{x}\, d\boldsymbol{\xi}}$ and an equation describing the propagation due to the free motion and collisions of such a distribution, the Boltzmann equation, in 1872. [3] Macroscopic variables like density and velocity emerge as expected values (moments) from the distribution. Since continuum-based flows are assumed to be close to equilibrium, the macroscopic behaviour for dense fluids ($Kn := l_{mfp}/L \to 0$), given by the Navier-Stokes equations, can be recovered by applying an asymptotic *perturbation analysis* ($\epsilon \propto Kn$), $f = \sum_{n=0}^{\infty} \epsilon^n f^{(n)}$ referred to as *Chapman-Enskog expansion*, [5] around the equilibrium $f^{(0)} := f^{(eq)}$ and recombining the conserved quantities.

After the success of the closely-related *cellular automata*, the framework of the Boltzmann equation was used to construct a physically consistent *fictional gas* with convenient numerical properties: [20] In the second-order accurate *lattice-Boltzmann* method (LBM) the Boltzmann equation is discretised in space $\mathcal{D} := \{x, y, z\}$ into regular velocity subsets, *lattices* $\mathcal{L} := \{\boldsymbol{c}_\alpha\}$, that only interact with their *nearest neighbourhood*, defined by $\Delta\boldsymbol{x}_\alpha := \{\Delta_t\, \boldsymbol{c}_\alpha\}$. The time Δ_t and spatial step Δ_x are chosen to unity ("lattice units") respectively and the populations now travel with a *single speed* $c := \Delta_x/\Delta_t$ on a discrete *equidistant grid* and collide with populations from neighbouring nodes. All continuous variables have to be mapped to discrete space while retaining exactness for the main hydrodynamic quantities. They may be constructed using expected values, moments of the discrete distribution functions,

$$\rho = \Delta^3 \sum_{\alpha \in \mathcal{L}} f_\alpha \qquad (2a) \qquad\qquad \rho_0 u_i = \Delta^3 \sum_{\alpha \in \mathcal{L}} c_{i\alpha} f_\alpha \qquad (2b)$$

where Δ is introduced as a velocity element for the consistency of physical units only: The sum reflects a quadrature of the continuous integral.
In this study the three-dimensional D3Q19-lattice [22] is used

$$\boldsymbol{c}_\beta = \begin{bmatrix} c_{x\beta} \\ c_{y\beta} \\ c_{z\beta} \end{bmatrix} = c \begin{bmatrix} 0 & 1 & 0 & 0 & 1 & 1 & 1 & 1 & 0 & 0 \\ 0 & 0 & 1 & 0 & 1 & -1 & 0 & 0 & 1 & 1 \\ 0 & 0 & 0 & 1 & 0 & 0 & 1 & -1 & 1 & -1 \end{bmatrix} \qquad (3)$$

where $\beta \in [0, 9]$ and their opposite directions $\boldsymbol{c}_{\overline{\beta}} = -\boldsymbol{c}_\beta$ for $\overline{\beta} \in [1, 9]$ form the 19 lattice velocities $\alpha := \{\beta, \overline{\beta}\}$. The length of different vectors $\boldsymbol{c}_\alpha$ is accounted for by weighting each direction with the corresponding weights

$$w_\beta = \begin{bmatrix} \frac{1}{3} & \frac{1}{18} & \frac{1}{18} & \frac{1}{18} & \frac{1}{36} & \frac{1}{36} & \frac{1}{36} & \frac{1}{36} & \frac{1}{36} & \frac{1}{36} \end{bmatrix}^T \qquad (4)$$

which can be interpreted as corrected particle masses. The resulting discrete evolution equation can be separated into two steps: The collision of all particle distributions at a node and the streaming to its neighbouring nodes. The collision step is modelled through a linear relaxation towards a *discrete Maxwell-Boltzmann equilibrium* obtained by a *low Mach number expansion* where - for consistency - the terms of higher order stemming from pressure fluctuations $\Delta p = (\rho - \rho_0)/c_s^2$ are neglected as well (incompressible equilibrium) [14]

$$f_\alpha^{(eq)}(\boldsymbol{x}, t) = \frac{w_\alpha}{\Delta^3} \Big[\rho + \rho_0 \Big(\frac{(\boldsymbol{c}_\alpha \cdot \boldsymbol{u})}{c_s^2} + \frac{(\boldsymbol{c}_\alpha \cdot \boldsymbol{u})^2}{2c_s^4} - \frac{\boldsymbol{u}^2}{2c_s^2} \Big) \Big] + \mathcal{O}(Ma^2). \qquad (5)$$

ICCS Camera Ready Version 2021
To cite this paper please use the final published version:
DOI: 10.1007/978-3-030-77980-1_19

$c_s := \sqrt{\left(\frac{\partial p}{\partial \rho}\right)_T} = \sqrt{R_m T}$ corresponds to the iso-thermal speed of sound of an ideal gas that in case of the most common discretisations can be found to correspond to $c_s = c/\sqrt{3}$. For the turbulent large-eddy simulations the BGK collision operator with a single relaxation time τ^+ [2]

$$f_\alpha(\boldsymbol{x} + \Delta_t\, \boldsymbol{c}_\alpha, t + \Delta_t) = f_\alpha(\boldsymbol{x}, t) + \frac{\Delta_t}{\tau^+}(f_\alpha^{(eq)} - f_\alpha) + \mathcal{O}(\Delta_x^2) + \mathcal{O}(\Delta_t^2) \tag{6}$$

was used while for the simulations considering laminar flow conditions the two-relaxation time (TRT) model was chosen [11], which applies an eigen-decomposition and relaxes even (+) and odd (−) hydrodynamic moments $\sum_\alpha c_{i\alpha}^n f_\alpha$ at individual rates τ^+ and τ^-.
Through a Chapman-Enskog expansion [14] the conservation equations for incompressible flow containing an error term $\mathcal{O}(Ma^3)$ can be found to govern this discrete system where the equation of state is given by $p = \rho c_s^2$ and the kinematic viscosity can be redefined absorbing the emerging discretisation error as

$$\nu = \frac{\mu}{\rho_0} = \left(\frac{\tau^+}{\Delta_t} - \frac{1}{2}\right) c_s^2 \Delta_t. \tag{7}$$

Now this numerical scheme can be used to *approximate the solution of incompressible fluid flows by allowing controlled compressibility.* Neglecting body forces the only characteristic number of relevance for single component fluid flow is the *Reynolds number* that is used to set the relaxation time by enforcing the viscosity $\nu_0 = (U\,L)\,/Re$. The corresponding temporal resolution is set by choosing the characteristic simulation velocity U within the stability limit $Ma = U/c_s << 1$. The simulation units can be converted to physical units according to the *law of similarity.*

Smagorinsky Large-Eddy Turbulence Model. The Smagorinsky *subgrid-scale model* is an eddy-viscosity based model, which applies low-pass filtering of the governing equations while smaller unresolved scales are modelled using an *additional isotropic dissipation*, the turbulent viscosity ν_T. As the explicit LBM algorithm on a regular grid naturally uses a high temporal and spatial resolution and furthermore the strain-rate can be calculated locally without interpolation (see equation 8)

$$S_{ij} := \frac{1}{2}\left(\frac{\partial u_i}{\partial x_j} + \frac{\partial u_j}{\partial x_i}\right) = -\frac{1}{2\rho_0 c_s^2 \tau} \Pi_{ij}^{(1)} + \mathcal{O}(Ma^3) \tag{8}$$

this model can be included fairly easily into an existing LBM simulation by including an additional local turbulent relaxation time τ_T (see equations 9 and 10, where C is the Smagorinsky parameter) [16].

$$\nu = \left(\frac{\tau}{\Delta_t} - \frac{1}{2}\right) c_s^2 \Delta_t = \underbrace{\left(\frac{\tau^+}{\Delta_t} - \frac{1}{2}\right) c_s^2 \Delta_t}_{\nu_0} + \underbrace{\tau_T\, c_s^2}_{\nu_T} \tag{9}$$

ICCS Camera Ready Version 2021
To cite this paper please use the final published version:
DOI: 10.1007/978-3-030-77980-1_19

$$\tau_T \approx \frac{1}{2}\left(\sqrt{\tau^{+\,2} + \frac{2\sqrt{2}(C\Delta_{\overline{x}})^2}{\rho_0 c_s^4}\sqrt{\sum_{i,j\in\mathcal{D}} \Pi_{ij}^{(1)}\,\Pi_{ij}^{(1)}}} - \tau^+\right) \tag{10}$$

The first-order contribution $\Pi_{ij}^{(1)}$ to the incompressible momentum flux tensor $\Pi_{ij} \coloneqq \rho u_i u_j - p\delta_{ij} + 2\mu S_{ij}$ is given by equation 11, where the first order contribution $f_\alpha^{(1)}$ is approximated by the entire non-equilibrium part $f_\alpha^{(neq)} \coloneqq f_\alpha - f_\alpha^{(eq)}$ from the previous time step.

$$\Pi_{ij}^{(1)} = \Delta^3 \sum_{\alpha\in\mathcal{L}} c_{i\alpha} c_{j\alpha} f_\alpha^{(1)} \tag{11}$$

2.2 LBM for Mass Transfer

The momentum equation can be seen as an advection-diffusion equation for the momentum with a corresponding "diffusion coefficient", the viscosity ν. Similarly an artificial algorithm exhibiting the desired macroscopic behaviour on a continuum level can be constructed for other quantities that could be seen as advected by a flow field and diffused. Similar to the hydrodynamic flow this can be done for the mass-fraction $\Upsilon \coloneqq m_{comp}/m_{tot}$ using a second population g_α while enforcing the basic property $\Upsilon \coloneqq \Delta^3 \sum_{\alpha\in\mathcal{L}} g_\alpha$. With a relatively simple Chapman-Enskog expansion [7] the following correlation of the diffusion coefficient and the anti-symmetric relaxation time λ^- may be found

$$D = \left(\frac{\lambda^-}{\Delta_t} - \frac{1}{2}\right) c_s^2 \Delta_t. \tag{12}$$

Such a scalar quantity can be useful to determine *dispersion properties of porous media*, e.g. by calculating the cumulative residence time distribution $F(t)$ by means of *virtual tracer step-experiments*.

Turbulent Scalar Transport. Analogous to turbulent fluid flows, also turbulent scalar transport leads to a closure problem. The simplest way of modelling the unknown term $\partial\overline{u_j'\Upsilon'}/\partial x_j$ [24] is by assuming an additional constant turbulent diffusion coefficient D_T that is modelled according to the *Reynolds analogy* with a *turbulent Schmidt number* $Sc_T \coloneqq 0.2 - 2.5$ [12], given in equation 13.

$$D_T \coloneqq \frac{\nu_T}{Sc_T} \tag{13}$$

Therefore we propose an extension to the advection-diffusion LBM in an analogous way to fluid flow with an additional turbulent relaxation time λ_T for mass-transfer (see equation 14).

$$D = \left(\frac{\lambda}{\Delta_t} - \frac{1}{2}\right) c_s^2 \Delta_t = \underbrace{\left(\frac{\lambda^-}{\Delta_t} - \frac{1}{2}\right) c_s^2 \Delta_t}_{D_0} + \underbrace{\lambda_T\, c_s^2}_{D_T} \tag{14}$$

ICCS Camera Ready Version 2021
To cite this paper please use the final published version:
DOI: 10.1007/978-3-030-77980-1_19

Based on these equations the *additional turbulent relaxation time for scalar transport* λ_T *equals to a rescaled turbulent relaxation time of the fluid flow* τ_T. Assuming an equal speed of sound of the hydrodynamic and diffusion lattice this results in equation 15.

$$\lambda_T = \frac{\tau_T}{Sc_T} \tag{15}$$

For the simulations the product of Smagorinsky constant and filter width is specified as $C\,\Delta_{\overline{x}} = 0.15$ while the laminar and turbulent Schmidt numbers are set to $Sc = 1$ and $Sc_T = 0.7$, respectively.

3 Porous Media - Simulation Domain

Confined flows in porous geometries are inherently different from free flows. Many characteristics such as velocity distributions depend on the precise bed morphology. For particle flows a specific Reynolds number, the particle Reynolds number, can be defined as

$$Re_p \coloneqq \frac{U\,D_s}{\nu_0} \tag{16}$$

where the characteristic velocity U is the unperturbed velocity at some distance from the particle and the characteristic length is the diameter of a sphere of equivalent volume D_s. To define the different flow regimes Dybbs and Edwards [6] introduced the interstitial Reynolds number $Re_\phi \coloneqq |\boldsymbol{u}|\,D_s/\nu_0$, which for isotropic media degenerates to $Re_\phi \approx Re_p/\phi$. The different regimes are then given by: *Viscous flow* ($Re_\phi \lesssim 1$), *steady laminar* inertial regime ($10 \lesssim Re_\phi \lesssim 150$), *unsteady laminar* inertial regime with oscillating behaviour ($150 \lesssim Re_\phi \lesssim 300$) and unsteady chaotic *turbulent* flow ($Re_\phi \gtrsim 300$).

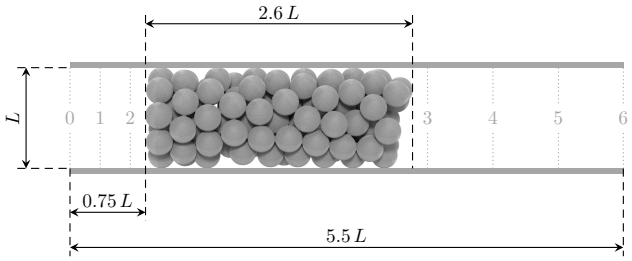

Fig. 1: Geometry made of spheres with its inlet (left) and six planes where the species mass fraction was tracked

Packed-bed of Spheres. In order to obtain an artificial porous medium, a tube ($D_t = 15\,\text{mm}$) was filled virtually with 105 spheres with a diameter of $D_s = 4\,\text{mm}$ leading to a tube-to-particle ratio $r_{tp} \coloneqq D_t/D_p$ of 3.75. For this purpose, the Packed Bed Generator PBG V.2 for Blender by B. Partopour and A.G. Dixon [21] was used. The generated geometry, resulting in a void fraction of $\phi = 0.45$, is displayed in figure 1. For the simulation with Fluent v19.2 the

ICCS Camera Ready Version 2021
To cite this paper please use the final published version:
DOI: 10.1007/978-3-030-77980-1_19

numerical grid consists of 8.5 million cells while for the LBM simulation meshes with a characteristic length of 146 and 196 lattice units were used. Tracer step-experiments were simulated at four different Reynolds numbers in the case of laminar viscous ($Re_p = 1$), steady laminar ($Re_p = 10$), unsteady transitional ($Re_p = 100$) and unsteady turbulent ($Re_p = 1000$) conditions. At the inlet a *block velocity profile* (in the LBM simulation with a characteristic velocity of $U_{lb} = 0.005$) was imposed in the form of a *Guo's non-equilibrium extrapolation boundary condition* [13] and a *Dirichlet boundary condition* (given concentration value) for the species with an *anti-bounce-back* boundary condition (ABB) [10]. At the outlet Guo's method was chosen to enforce a *constant pressure* and the *copying of all the populations* of the neighbouring fluid node was used to impose a second-order accurate *zero-gradient outlet* for the mass transfer population. Solid walls were modelled for both, the fluid flow and the species, with *half-way bounce-back* (HW-BB) [15].

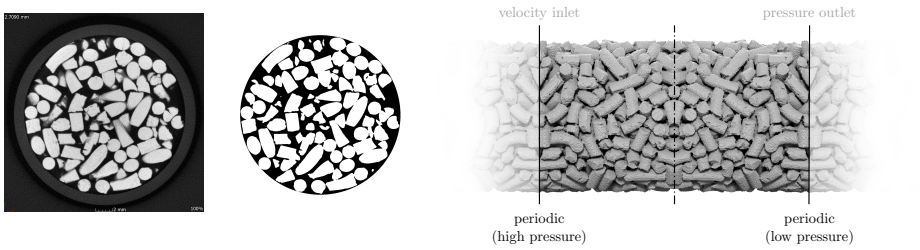

Fig. 2: Subfigure a: Cross-section of the adsorber using μCT scanning technique (left) and post-processed image (right), Subfigure b: Resulting computational domain obtained by mirroring and boundary conditions for the adsorber with about 11 million nodes

Realistic Adsorber Geometry. The second geometry considered with the LBM was a realistic adsorber bed made of hopcalite pellets. Cross-sections of the adsorber were obtained using μCT scans as given in figure 2a. The pellets are irregular cylinders with a diameter of approx. 1.12 mm and heights that vary between 0.83 mm and 3.88 mm (average 2.12 mm, standard deviation 0.74 mm), conforming to a tube-to particle ratio r_{tp} of around 13.39. The average equivalent spherical diameter (diameter of a sphere with the same volume as the particle) corresponds to $D_s = 1.56$ mm. Grid generation for a simulation based on FVM (Fluent v19.2) was no longer possible, however the regular grid applied in the LBM was created by voxelising the scans of the cross-sections. Ideally one would use periodic boundary conditions to determine the transport properties of such porous media. However, this is generally not possible as start and end do not fit neatly together. We therefore mirrored the domain as can be seen in figure 2b resulting in an undisturbed flow field with a constant void fraction. In order to obtain a realistic periodic simulation we started the simulation with a *constant*

ICCS Camera Ready Version 2021
To cite this paper please use the final published version:
DOI: 10.1007/978-3-030-77980-1_19

velocity inlet and pressure outlet at a given Reynolds number of $Re_p \approx 5$, calculated the pressure drop due to the porous medium and then imposed *periodic pressure drop boundaries* according to Kim and Pitsch [19]. This lead to a realistic velocity profile as well as an accurate pressure drop corresponding to the chosen particle Reynolds number.

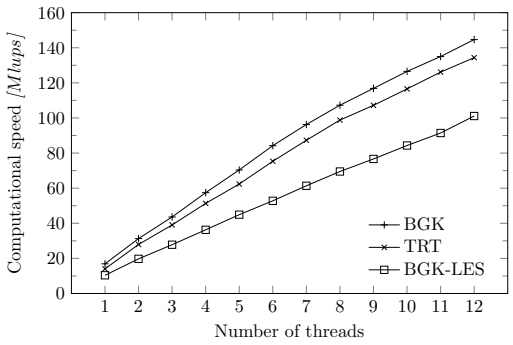

Fig. 3: Parallel scaling in million double-precision lattice updates per second (Mlups) of the proposed implementation for a three-dimensional lid-driven cavity and a $D3Q19$-lattice on a 12-core desktop system for different collision operators

Computational Framework. The simulations were performed on a *shared memory system* with a proprietary multi-threaded OpenMP C++17 framework that makes use of several optimisations: *Grid merging* for multiple interacting populations is combined with a *row-major linear memory layout* and additional optional array *padding* to match the cache line size of 64 Bytes and minimise false sharing. The padding can also be used to store a *logical mask for sparse domains* such as the considered porous media. For more predictable branch prediction behaviour every cell (if not excluded by the logical mask) performs collision and streaming while boundary conditions are imposed locally afterwards. In order to reduce the memory bandwidth for the memory-bound LBM algorithms an *A-A access pattern*, [1] where even time steps perform local collisions with a reverse read and odd steps a combined streaming-collision-streaming step with a reverse write, and 3-way spatial *loop blocking* were introduced. Furthermore to maximise the performance all these features were implemented by means of macros, templates and inline functions which are already known to the compiler at compilation time. With this implementation on a *twelve-core* Intel i9-7920X *processor* for all collision operators a *parallel scalability* of *around 90%* was obtained (see figure 3). A reduced framework for generic lattices that uses these optimisations and additionally manual AVX2/AVX512 vector intrinsics implementations can be found on the Github repository https://github.com/2b-t/LB-t.

4 Results and Discussion

In this section the results obtained with the in-house LBM code and FVM-based Fluent are compared with special consideration of the species transport within

ICCS Camera Ready Version 2021
To cite this paper please use the final published version:
DOI: 10.1007/978-3-030-77980-1_19

the packed-bed domain (see section 4.1). Simulations in the packed-bed were carried out under laminar, transitional and turbulent flow regime. Since many previous studies focused on scalar transport under laminar conditions, the results presented here are focused on the turbulent fluid flow and species transport, where the applicability of modelling the turbulent scalar transport using an additional turbulent relaxation time for the mass transfer were validated. In section 4.2 the LBM is also applied for the simulation within a adsorber, where a simulation with the FVM was no longer possible, again highlighting the advantage of the LBM for complex geometries.

4.1 Packed-bed of Spheres

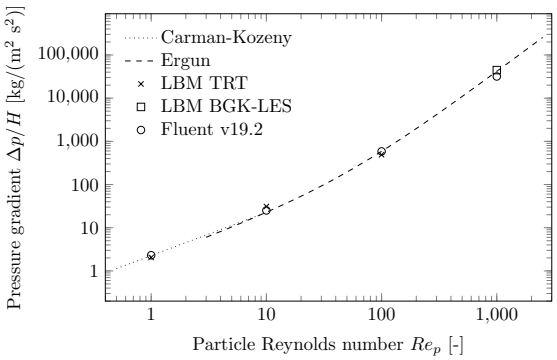

Fig. 4: Pressure drop in the packed-bed of spheres

Within this section the simulation results will be analysed considering the (i) pressure drop in the domain, (ii) the velocity profile and (iii) observation of the species concentrations at the 6 planes depicted in figure 1.

Pressure Drop. The pressure drop caused by the porous domain was tracked (see figure 4) and compared to the *empirical correlations* proposed by *Carman-Kozeny* and *Ergun* (approaches are summarized in [23]). For all considered Reynolds numbers the pressure drops determined with LBM correspond well with the empirical correlations and the Fluent simulations. For the LBM simulations up to the transitional state ($Re_p = 100$) the TRT model was used while for $Re_p = 1000$ the LES model was necessary to keep the simulations stable and describe the unresolved scales. For the FVM simulations at the highest Reynolds number the commercial software Fluent with a $k - \omega$ URANS turbulence model was used. In all simulations the computation time of the two approached was similar but the LBM simulations naturally required a time-step that is 60 times smaller and therefore the much more accurate large-eddy turbulence model can be used at virtually no additional cost. A FVM large-eddy simulation on the other hand is not computationally feasible in particular on consumer-grade hardware like the one used in terms of this study.

ICCS Camera Ready Version 2021
To cite this paper please use the final published version:
DOI: 10.1007/978-3-030-77980-1_19

Velocity Profile. In order to analyse the flow properties inside the porous medium the time-averaged instantaneous velocity distributions for each particle Reynolds number were calculated. For all Reynolds numbers we obtained *peak axial velocities* that are around *twelve times higher* than the inlet velocity and radial velocities that are roughly six times higher than the inlet velocity (see also figure 5). Furthermore, while for low Reynolds number flow some parts of the fluid might move slowly while others move significantly faster, only around 1.5% of the fluid inside the porous medium move in opposite direction to the main flow. With rising Reynolds number the fraction of backflow rises to up to 14% of the entire porous bed at $Re_p = 1000$. Furthermore the flow becomes increasingly unsteady: macroscopic eddies and dead water emerge, in particular behind the porous medium (see figure 5). For $Re_p = 100$ the exit behind the porous medium becomes visually unsteady and for $Re_p = 1000$ also turbulent fluctuations inside the porous medium can be observed.

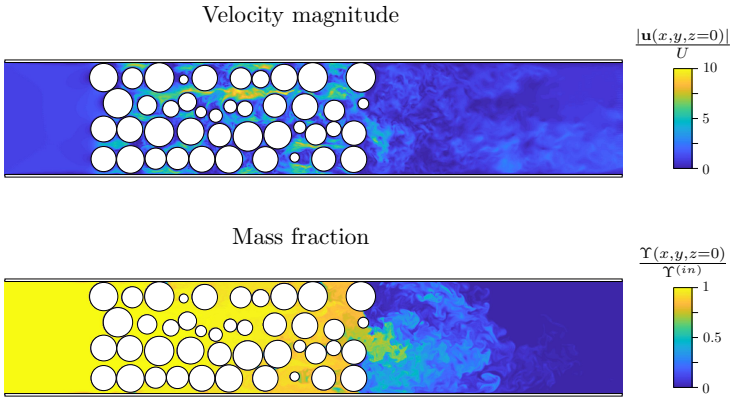

Fig. 5: Normalised instantaneous velocity field (top) and mass fraction (bottom) in a cross-section of the large-eddy LBM simulation for $Re_p = 1000$

Species Transport in the Packed-bed Domain. Axial Péclet numbers for gaseous flows are known to be of the magnitude of the molecular diffusion. Commonly in the literature values around $Pe_{ax} \approx 2$ are found. This leads to curves of the mass fractions that in dimensional coordinates are comparably similar in shape almost independent of the Reynolds number (see figure 6). The turbulent fluctuations and macroscopic eddies lead to fluctuations in the mass fractions but the trend of the mass fraction closely resembles the ones generated by the Fluent simulations for the two considered Reynolds numbers $Re_p = 10$ and $Re_p = 1000$.

4.2 Realistic Adsorber Geometry

Since the μCT scan of this particular porous medium is characterised by a higher void fraction in one corner of the domain, the LBM simulation showed an in-

ICCS Camera Ready Version 2021
To cite this paper please use the final published version:
DOI: 10.1007/978-3-030-77980-1_19

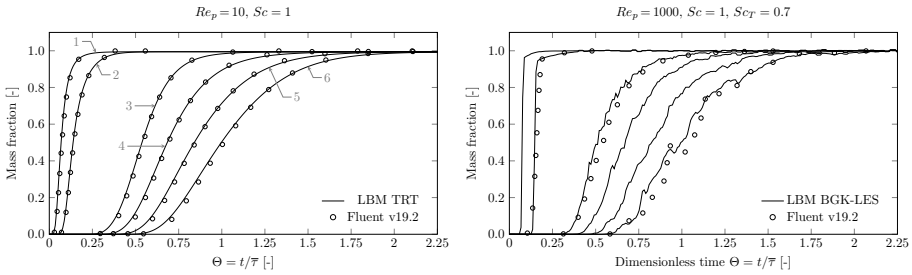

Fig. 6: Mass-flow averaged cumulative residence time distribution $F(t)$ over dimensionless time Θ (where $\overline{\tau}$ is the mean residence time) at different cross-sections obtained by LBM (solid lines) and Ansys Fluent (markers) for two different particle Reynolds numbers Re_p

creased species transport in this region (see red box in figure 7). Due to mass continuity the higher mass flow in the short-circuit region leads to a stagnant flow in the center of the bed. This effect represents a significant deviation from the ideal plug flow, assumed in many simplified models to predict the species transport in porous media. To reveal such effects, advanced simulation methods such as the proposed LBM model are necessary. The backflow across the entire porous medium was found to only account for 1.29% of the fluid cells for the considered Reynolds number of $Re_p \approx 5$.

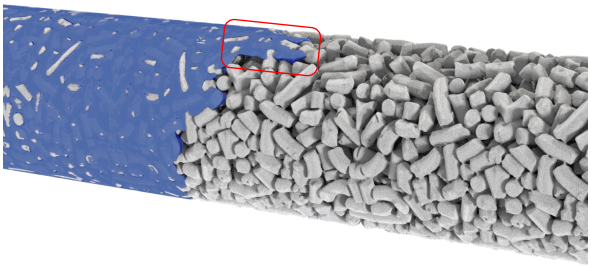

Fig. 7: Instantaneous iso-mass fraction $\Upsilon = 0.6$ in realistic adsorber geometry obtained my mirroring for $Re_p \approx 5$ - A short-circuit (red box) leading to a bi-modal distribution is clearly visible on top.

5 Conclusion and Outlook

In the present paper the lattice-Boltzmann method was applied to a packed-bed of spheres and an adsorber geometry for the case of *laminar, transitional and turbulent flows* in the range from $Re_p = 1$ to $Re_p = 1000$. In the process the *Smagorinsky large-eddy turbulence model in LBM was extended to account for*

ICCS Camera Ready Version 2021
To cite this paper please use the final published version:
DOI: 10.1007/978-3-030-77980-1_19

turbulent diffusion by rescaling the turbulent relaxation time for hydrodynamic flow with a turbulent Schmidt number and it was briefly outlined how a suitable simulation domain for periodic pressure boundaries can be obtained by mirroring the μCT scan. The obtained results agreed well with the empirical correlations for the *pressure drop* and the species transport predicted by the commercial software Fluent. The application of LBM clearly reaches far beyond the laminar simulations in the creeping and low-Reynolds number regime and is a powerful tool for transitional and turbulent simulations inside porous media.

References

1. Bailey, P., Myre, J., Walsh, S., Lilja, D., Saar, M.: Accelerating Lattice-Boltzmann Fluid Flow Simulations Using Graphics Processors. pp. 550–557 (Sep 2009). https://doi.org/10.1109/ICPP.2009.38
2. Bhatnagar, P.L., Gross, E.P., Krook, M.: A Model for Collision Processes in Gases. I. Small Amplitude Processes in Charged and Neutral One-Component Systems. Physical Review **94**(3), 511–525 (May 1954). https://doi.org/10.1103/PhysRev.94.511
3. Boltzmann, L.: Weitere Studien über das Wärmegleichgewicht unter Gasmolekülen. In: Brush, S.G. (ed.) Kinetische Theorie II: Irreversible Prozesse Einführung und Originaltexte, pp. 115–225. WTB Wissenschaftliche Taschenbücher, Vieweg+Teubner Verlag, Wiesbaden (1970). https://doi.org/10.1007/978-3-322-84986-1_3
4. Caulkin, R., Jia, X., Fairweather, M., Williams, R.: Predictions of Porosity and Fluid Distribution through Nonspherical-packed Columns. AIChE Journal **58** (05 2012). https://doi.org/10.1002/aic.12691
5. Chapman, S., Cowling, T.G., Burnett, D.: The Mathematical Theory of Nonuniform Gases: An Account of the Kinetic Theory of Viscosity, Thermal Conduction and Diffusion in Gases. Cambridge University Press (1990)
6. Dybbs, A., Edwards, R.V.: A New Look at Porous Media Fluid Mechanics Darcy to Turbulent. In: Bear, J., Corapcioglu, M.Y. (eds.) Fundamentals of Transport Phenomena in Porous Media, pp. 199–256. NATO ASI Series, Springer Netherlands, Dordrecht (1984). https://doi.org/10.1007/978-94-009-6175-3_4
7. Flekkøy, E.G.: Lattice Bhatnagar-Gross-Krook Models for Miscible Fluids. Physical Review E **47**(6), 4247–4257 (Jun 1993). https://doi.org/10.1103/PhysRevE.47.4247
8. Freund, H., Bauer, J., Zeiser, T., Emig, G.: Detailed Simulation of Transport Processes in Fixed-beds. Industrial & Engineering Chemistry Research **44**(16), 6423–6434 (2005). https://doi.org/10.1021/ie0489453
9. Geier, M., Sch M.: The Cumulant Lattice-Boltzmann Equation in Three Dimensions: Theory and Validation. Computers & Mathematics with Applications **70**(4), 507 – 547 (2015). https://doi.org/https://doi.org/10.1016/j.camwa.2015.05.001
10. Ginzburg, I.: Generic Boundary Conditions for Lattice-Boltzmann Models and Their Application to Advection and Anisotropic Dispersion Equations. Advances in Water Resources **28**(11), 1196–1216 (Nov 2005). https://doi.org/10.1016/j.advwatres.2005.03.009
11. Ginzburg, I.: Two-relaxation-time Lattice-Boltzmann Scheme: About Parametrization, Velocity, Pressure and Mixed Boundary Conditions. Communications in Computational Physics **3**, 427–478 (Jan 2008)

ICCS Camera Ready Version 2021
To cite this paper please use the final published version:
DOI: 10.1007/978-3-030-77980-1_19

12. Gualtieri, C., Angeloudis, A., Bombardelli, F., Jha, S., Stoesser, T.: On the Values for the Turbulent Schmidt Number in Environmental Flows. Fluids **2**(2), 17 (Jun 2017). https://doi.org/10.3390/fluids2020017
13. Guo, Z.L., Zheng, C.G., Shi, B.C.: Non-equilibrium Extrapolation Method for Velocity and Pressure Boundary Conditions in the Lattice-Boltzmann Method. Chinese Physics **11**(4), 366–374 (Mar 2002). https://doi.org/10.1088/1009-1963/11/4/310
14. He, X., Luo, L.S.: Lattice-Boltzmann Model for the Incompressible Navier-Stokes Equation. Journal of Statistical Physics **88**(3), 927–944 (Aug 1997). https://doi.org/10.1023/B:JOSS.0000015179.12689.e4
15. He, X., Zou, Q., Luo, L.S., Dembo, M.: Analytic Solutions of Simple Flows and Analysis of Non-slip Boundary Conditions for the Lattice-Boltzmann BGK Model. Journal of Statistical Physics **87**(1), 115–136 (Apr 1997). https://doi.org/10.1007/BF02181482
16. Hou, S., Sterling, J., Chen, S., D. Doolen, G.: A Lattice-Boltzmann Subgrid Model for High Reynolds Number Flows. Fields Inst. Commun. **6** (Feb 1994)
17. Jurtz, N., Kraume, M., Wehinger, G.D.: Advances in Fixed-bed Reactor Modeling using Particle-resolved Computational Fluid Dynamics (CFD). Reviews in Chemical Engineering **35**(2), 139–190 (2019). https://doi.org/10.1515/revce-2017-0059
18. Karlin, I.V., Gorban, A.N., Succi, S., Boffi, V.: Maximum Entropy Principle for Lattice Kinetic Equations. Physical Review Letters **81**(1), 6–9 (Jul 1998). https://doi.org/10.1103/PhysRevLett.81.6
19. Kim, S., Pitsch, H.: A Generalized Periodic Boundary Condition for Lattice-Boltzmann Method Simulation of a Pressure-driven Flow in a Periodic Geometry. Physics of Fluids **19** (Oct 2007). https://doi.org/10.1063/1.2780194
20. McNamara, G.R., Zanetti, G.: Use of the Boltzmann Equation to Simulate Lattice-Gas Automata. Physical Review Letters **61**(20), 2332–2335 (Nov 1988). https://doi.org/10.1103/PhysRevLett.61.2332
21. Partopour, B., Dixon, A.G.: An Integrated Workflow for Numerical Generation and Meshing of Packed-beds of Non-spherical Particles: Applications in Chemical Reaction Engineering. 2017 AIChE Annual Meeting (Nov 2017)
22. Qian, Y.H., D'Humières, D., Lallemand, P.: Lattice BGK Models for Navier-Stokes Equation. Europhysics Letters (EPL) **17**(6), 479–484 (Feb 1992). https://doi.org/10.1209/0295-5075/17/6/001
23. Rhodes, M.: Introduction to Particle Technology. Wiley, Chichester, England; Hoboken, NJ, 2nd edn. (Apr 2008)
24. Roberts, P.J.W., Webster, D.R.: Turbulent Diffusion. Environmental Fluid Mechanics: Theories and Applications pp. 7–45 (2002), `https://cedb.asce.org/CEDBsearch/record.jsp?dockey=0277542`
25. Uphoff, S.: Development and Validation of Turbulence Models for Lattice-Boltzmann Schemes. Ph.D. Thesis, Technische Universität Braunschweig (Jan 2013), `https://publikationsserver.tu-braunschweig.de/receive/dbbs_mods_00055260`
26. Zeiser, T., Steven, M., Freund, H., Lammers, P., Brenner, G., Durst, F., Bernsdorf, J.: Analysis of the Flow Field and Pressure Drop in Fixed-bed Reactors with the Help of Lattice-Boltzmann Simulations. Philosophical transactions. Series A, Mathematical, Physical, and Engineering Sciences **360**, 507–520 (04 2002). https://doi.org/10.1098/rsta.2001.0945

ICCS Camera Ready Version 2021
To cite this paper please use the final published version:
DOI: 10.1007/978-3-030-77980-1_19